

---

# Dynamic Feature Selection based on Rule-based Learning for Explainable Classification with Uncertainty Quantification

---

Javier Fumanal-Idocin<sup>1</sup>, Raquel Fernandez-Peralta<sup>2</sup>, Javier Andreu-Perez<sup>1</sup>

<sup>1</sup> University of Essex, <sup>2</sup> Slovak Academy of Sciences

## Abstract

Dynamic feature selection (DFS) offers a compelling alternative to traditional, static feature selection by adapting the selected features to each individual sample. This provides insights into the decision-making process for each case, which makes DFS especially significant in settings where decision transparency is key, i.e., clinical decisions. However, existing DFS methods use opaque models, which hinder their applicability in real-life scenarios. DFS also introduces new own sources of uncertainty compared to the static setting, which is also not considered in the existing literature. In this paper, we formalize the additional sources of uncertainty in DFS, and give formulas to estimate them. We also propose novel approach by leveraging a rule-based system as a base classifier for the DFS process, which enhances decision interpretability compared to neural estimators. Finally, we demonstrate the competitive performance of our rule-based DFS approach against established and state-of-the-art greedy and reinforcement learning methods, which are mostly considered opaque, compared to our explainable rule-based system.

## 1 Introduction

Many real-world decision-making scenarios involve prohibitively high-dimensional information spaces, where acquiring all possible data is unfeasible due to cost or time constraints [Erion et al., 2022]. Consider, for instance, a doctor diagnosing a patient. The doctor must select only the right clinical trials to conduct, as they are expensive in terms of both money and time, which are usually scarce resources. Only a small subset will be truly relevant in accurately diagnosing the patient’s specific condition, and this subset will be different for each patient. The most intuitive and effective approach in such situations is to adapt the information acquisition process to the subject’s condition. This methodology, where features are acquired dynamically based on their evolving relevance is commonly referred to as Dynamic Feature Selection (DFS) [Melville et al., 2004].

The existing machine learning literature on DFS primarily explores two main approaches: reinforcement learning (RL) [Liu et al., 2021, Janisch et al., 2019] and greedy optimization [Chen et al., 2015]. RL-based approaches offer the potential to discover optimal policies for feature acquisition, but they come with the inherent challenges of RL training, including significant computational demands and potential convergence issues [Erion et al., 2022]. Greedy optimization methods maximize a measure that relates the known inputs with the response variable [Chattopadhyay et al., 2023, Takahashi et al., 2025]. Usually, this measure is the conditional mutual information (CMI) between input variables and the response variable, which has some desirable qualities in terms of uncertainty and prediction power [Gadgil et al., 2023]. This approaches also circumvent the issue of selecting a discrete variable in a neural network, which has non-differentiability issues Covert et al. [2023].

Significant research within CMI-based DFS methods focuses on the task of accurately estimating CMI itself, which often requires strong prior assumptions about the data distribution. It is possible to use a generative model to learn the feature distribution, which makes the CMI estimation straightforward [Ma et al., 2018], though it is computationally expensive to train and leads to slow inference. More recent research has also proposed gradient-based optimization with a neural regressor for CMI estimation, which does not use expensive generative models, using a value network with a loss function that recovers CMI at optimality [Gadgil et al., 2023]. Other greedy strategies bypass direct CMI computation, focusing instead on identifying the feature with maximum CMI without explicitly calculating its value [Covert et al., 2023]. Besides the feature selection process, it is also necessary to train a model that works well on any feature subset. Subset-adaptive mechanisms are popular for this task, as they allow partial specialization while retaining shared knowledge across subsets. Examples of this approach are hierarchical or modular parametrizations Rebuffi et al. [2018], mixture-of-experts architectures Shazeer et al. [2017], or meta-learning strategies Finn et al. [2017], Ha et al. [2017].

Despite the clear benefits of DFS in budget-sensitive scenarios, existing methods have struggled with two major limitations that hinder their widespread application in real-life environments:

- **Incomplete Uncertainty Quantification:** Existing DFS methods use value functions to guide feature selection based on predictive performance, but they do not quantify uncertainty in their decisions. Specifically, they ignore the epistemic uncertainty introduced by adapting models to different feature subsets, and the calibration during sequential acquisition. This limits their applicability in risk-sensitive domains requiring reliable confidence estimates.
- **Lack of interpretability:** DFS methods rely on neural-based classifiers, making individual predictions opaque even when the feature selection policy is interpretable. For example, suppose we want to analyse the impact of each feature in the final classification. This is problematic for adoption of DFS in real life decision-making.

In this paper, we address both limitations. First, we formalize the additional sources of uncertainty in DFS and how they affect DFS classifiers. Second, we propose a model agnostic DFS policy compatible with interpretable rule-based classifiers. Our contributions are:

- We formalize and quantify the additional sources of uncertainty that arise in DFS. We analytically characterize epistemic uncertainty from model adaptation to different feature subsets, challenges in estimating aleatoric uncertainty during sequential acquisition, and the problems of establishing an equivalence between prediction entropy and confidence when acquiring more information.
- We develop a complete rule-based DFS framework consisting of an adapted rule-based classifier that handles arbitrary feature subsets through condition removal and confidence re-estimation, and model-agnostic feature selection policy that greedily minimizes prediction divergence from the original model.
- We validate our approach on five datasets with variable feature costs, achieving competitive accuracy against state-of-the-art methods while providing superior interpretability. Our analysis reveals that existing DFS methods suffer from poor calibration despite high confidence, and that uncertainty reduction is primarily driven by information accumulation rather than selection strategy.

## 2 Uncertainty Quantification in Dynamic Feature Selection

**Notation and Problem Formulation.** Let  $\mathbf{x} = (x_1, \dots, x_M)$  be an input feature vector and  $y \in \{1, \dots, C\}$  a corresponding target label in a supervised learning paradigm. The complete set of  $N$  input samples is denoted as  $X = \{\mathbf{x}^1, \dots, \mathbf{x}^N\}$ . A partially observed sample, where only features indexed by  $S$  have been observed, is denoted as  $\mathbf{x}_S = \{x_i : i \in S\}$ . The set of unobserved features is denoted as  $\bar{S} = \{1, \dots, M\} \setminus S$ .

**Uncertainty Quantification in Machine Learning.** Following the taxonomy given in Hüllermeier and Waegeman [2021], uncertainty can be categorized into two main categories. Aleatoric Uncertainty is the inherent irreducible noise in the data-generating process. This could be inherent to the analysed process, i.e., tossing a coin, noise in the measurements, etc. Epistemic Uncertainty is

the model’s uncertainty due to a lack of knowledge about the optimal parameters  $\theta$ , which can be reduced with more data.

DFS introduces complications to this standard taxonomy. Unlike static feature selection where uncertainty is assessed once on complete data, DFS requires uncertainty quantification at every step of the sequential process, with predictions made on different feature subsets  $\mathbf{x}_S$  for each sample. This creates new sources of uncertainty and changes how existing sources manifest, which we analyse in the following subsections.

## 2.1 Model Adaptation creates Epistemic Uncertainty

In the DFS literature, the classifier parameters,  $\theta$ , are usually trained using the following expression Gadgil et al. [2023]:

$$\theta^* = \arg \min_{\theta} \mathbb{E}_S \mathbb{E}_{\mathbf{x}, y} l(f_{\theta}(\mathbf{x}_S), y), \quad (1)$$

where  $f_{\theta}$  denotes a model capable of making predictions given any subset of features  $S$ . In practice, this is usually implemented by training a model that has access to all features, while treating the features not included in  $S$  as unknown. To evaluate  $f_{\theta}(\mathbf{x}_S)$ , these missing features are typically handled through some form of imputation method, such as zero/mean or conditional expectation imputation. Notice that this introduces an imputation bias between the best predictor on complete data and that on imputed inputs. Although solving Eq. (1) results in a parameter configuration that minimizes the expected loss across all possible subsets, the resulting model may differ from a local model trained exclusively on a particular subset of features with an equivalent training objective:

$$\theta_S^* = \arg \min_{\theta_S} \mathbb{E}_{\mathbf{x}, y} l(f_{\theta_S}(\mathbf{x}_S), y). \quad (2)$$

If we measure the risk of a model on subset  $S$  as  $\mathcal{R}_S(f) = \mathbb{E}_{\mathbf{x}, y} l(f(\mathbf{x}_S), y)$ , we can expect both models to have different risks. We measure the discrepancy of  $f_{\theta^*}$  and  $f_{\theta_S^*}$  as their difference in risk:

$$\Delta_S = \mathcal{R}_S(f_{\theta^*}) - \mathcal{R}_S(f_{\theta_S^*}). \quad (3)$$

A positive  $\Delta_S$  indicates that the globally trained model  $f_{\theta^*}$  performs worse on the specific subset  $S$  than a hypothetical local optimum  $f_{\theta_S^*}$ , reflecting a loss of specialization caused by averaging across subsets in Eq. (1). Conversely,  $\Delta_S \approx 0$  implies that  $f_{\theta^*}$  generalizes well to  $S$ , achieving near-optimal performance despite joint training.

The exponential growth of the feature subset space,  $2^M$ , forces  $\theta^*$  to balance many local optima and unseen feature subsets, which may lead to a positive and sometimes large  $\Delta_S$  due to limited capacity for subset-specific adaptation. This produces predictions of uneven quality depending on the  $S$  available, as the epistemic uncertainty in those subsets with large  $\Delta_S$  will be high. This challenge is analogous to the core problem in Invariant Risk Minimization Krueger et al. [2021], where each subset  $S$  is treated as a distinct “environment”. The issue is mitigated in DFS by using two different strategies. The first is to pre-train the classifier using random feature subsets Rangrej and Clark [2021]. The second is jointly train a feature selector model and a classifier. So, instead of sampling uniformly  $S$ , they train the model sampling features from the selector model  $q_{\phi}$ , given the already observed features. This changes Eq. (1) into:

$$\theta^* = \arg \min_{\theta} \mathbb{E}_{\mathbf{x}, y} \mathbb{E}_{S \sim q_{\phi}(\cdot | \mathbf{x})} l(f_{\theta}(\mathbf{x}_S), y). \quad (4)$$

However, this approach also introduces important limitations. The selector  $q_{\phi}$  may explore only a small fraction of all possible feature subsets  $S$ , which may bias the predictor’s accuracy toward the frequently selected ones. This results in a trade-off where predictive power is diminished for non and rarely selected subsets. Moreover, this scheme is effective when the predictor guides the feature selection process, but it may become vulnerable to changes in external factors. For example, when relevant variables needed by the selector  $q_{\phi}$  are unavailable for certain samples, or when the selector itself is giving poor estimates of the utility of the features.

## 2.2 Estimating Aleatoric Uncertainty during Sequential Acquisition

The ideal DFS classifier should estimate  $p(y | \mathbf{x}_S)$  for every  $S$  in the query process:

$$p(y | \mathbf{x}_S) = \int_{\mathbf{x}_{\bar{S}}} p(y | \mathbf{x}_S, \mathbf{x}_{\bar{S}}) p(\mathbf{x}_{\bar{S}} | \mathbf{x}_S) d\mathbf{x}_{\bar{S}}. \quad (5)$$

Generally speaking, DFS methods do not suffer from information leakage, which could affect this estimation Oosterhuis et al. [2024], because by definition of DFS, all decisions must be taken only with observed information. However, many classical imputation methods for the unobserved features can bias this estimation. For example, if we use the classical mean imputation method, we are implicitly assuming a degenerate distribution where the unobserved features are fixed at their expected values,  $\mu(\mathbf{x}_{\bar{S}})$ . Consequently, Eq. (5) simplifies to  $p(y | \mathbf{x}_S, \mathbf{x}_{\bar{S}} = \mu(\mathbf{x}_{\bar{S}}))$ , which biases the prediction. More sophisticated imputation mechanisms attempt to estimate  $p(\mathbf{x}_{\bar{S}} | \mathbf{x}_S)$  to better approximate Eq. (5). However, the quality of this approximation depends on how well the missing variables can be estimated from the seen ones, and how well that relationship can be learned from the actual data.

In previous DFS literature, there have been two options to solve this issue. One is to use a generative model to estimate  $p(\mathbf{x}_{\bar{S}} | \mathbf{x}_S)$  [Ma et al., 2018]. However, this approach requires a lot of data to work properly and tends to overfit. The alternative approach consists of imputing the missing values in  $\mathbf{x}_{\bar{S}}$  with a constant, typically zero. If the data is normalized, this zero imputation corresponds to the mean. The input to the classifier is then modified by concatenating the observed feature vector with a binary mask that explicitly indicates which features are observed and which are missing. This technique allows the model to differentiate between a truly zero value and an unobserved feature. It works similarly to imputation models, as it uses the mask to estimate the contribution of the missing values to the final prediction.

### 2.3 Non-Monotonicity of Uncertainty in Feature Acquisition

Given that the target conditional distribution  $p(y | \mathbf{x}_S)$  changes with the actively chosen feature subset  $S$ , the notion of a fixed, irreducible aleatoric uncertainty becomes problematic. For any subset  $S$  that is not the full feature set, additional features can be queried. Intuitively, decisions with more features should lead to more confident estimates. However, there are two considerations worth keeping in mind when querying more features.

First, gaining more information does not always result in more confident estimates of the model, not even in a perfectly trained one. For example, consider the classical example of diagnosing a rare disease (0.1% prevalence) through the perspective of DFS. If we do not perform any test, the probability distribution for the outcome is highly skewed (99.9% No Disease, 0.1% Disease). The model’s prediction is highly confident in this case. If we perform the test, the resulting outcome probability may be closer to 50/50 after observation, being less confident than before. This means that using, for example, metrics of prediction entropy or thresholds in class scores to stop querying is not a reliable policy Janisch et al. [2019], Yoon et al. [2018].

Second, although the intuition is that a decision made with the  $S \cup \{i\}$  feature set should be more trustworthy than one made with  $S$ , this holds only if the monotonicity condition  $\mathcal{R}_{S \cup \{i\}}(f_{\theta^*}) \leq \mathcal{R}_S(f_{\theta^*})$  is satisfied. The satisfaction of this condition is highly dependent on the problem structure. In complex scenarios monotonicity often fails, which is why static feature selection remains relevant and competitive Nogueira et al. [2018], Li et al. [2017]. Returning to the diagnostic example, a new test is only useful if its results can be correctly interpreted and if it genuinely contributes to diagnosing the disease. In DFS, this issue is mitigated by the use of the feature selector, which is suppose to only query useful information for the model. However, if the selector becomes unreliable or changes, this might become an issue.

## 3 A Dynamic Feature Selection Procedure for Rule-Based Models

The training of rule-based models has traditionally relied on greedy algorithms and heuristics, which presents a challenge for directly optimizing the global DFS objective in Eq. (1) compared to standard gradient-based methods. While traditional heuristic methods can be adapted to the DFS setting (see Appendix A), the computational overhead is significant.

Instead, we propose an alternative approach: we use a precomputed rule-based model trained on the full feature set, which we denote the “global model”. Then, we adapt this model to arbitrary

feature subsets rather than learning a specific model for DFS. This process sacrifices subset-specific performance, which induces epistemic uncertainty, but we mitigate this through feature selection policies that prioritize querying features where the adapted model is most reliable.

In the following, we discuss how a rule-based model is adapted for an arbitrary feature subset, and how this DFS feature selection policy works.

### 3.1 Adapting a rule-based model for DFS

We consider that the global model is a rule-based model trained on the entire set of features using any standard rule learning algorithm. Note that this model is not necessarily using all features; it can be trained using static feature selection or any other training technique. We shall refer to the prediction of the global model as  $p(\hat{y}|\mathbf{x})$ , and to the prediction done by any sub-model  $f_{\theta_S}$  on the  $S$  feature index set as  $p(\hat{y}|\mathbf{x}_S)$ .

We need to adapt this model to work with any feature subset  $S$ . We can easily do that by removing the conditions regarding the missing features, and removing rules that have no active conditions. Then, we re-estimate the predictions of each rule for each class. This ensures that the predictions are an unbiased estimate of the true conditional probability  $p(y | \mathbf{x}_S)$ , otherwise, we would be considering the missing conditions as true. This re-estimation is straightforward because we can compute we can easily compute the predictive power of any rule  $r_A \Rightarrow c$  measuring its confidence. As long as the length of the rule antecedent is reasonable e.g., less than four conditions, we can cache these values for all sub-rules to avoid any computational overhead in inference time. The main limitation of this approach is that the risk of the resulting sub-model can be high, as the original model was not trained to optimize performance on arbitrary feature subsets. In practice, we can mitigate this issue by using a suitable feature selection policy that prioritizes querying features that reduce epistemic uncertainty in the resulting model.

### 3.2 Defining the DFS policy given a global model

Our DFS policy assumes we have access to the rule-based global model defined in the previous section. It approximates the global model’s predictions for each sample using a greedy approach. For that, we define a value function,  $v_q(i, \mathbf{x}_S)$ , that computes the expected added value of adding the feature  $i$  given the currently observed  $\mathbf{x}_S$ . At each step of the DFS, we compute this expression for each unobserved feature, and query the feature with the highest value, up until the budget for the sample is exhausted.

To compute  $v_q(i, \mathbf{x}_S)$  we use a function  $q(x_i, \mathbf{x}_S)$  that quantifies the improvement of the prediction quality of  $f_{\theta, S \cup \{i\}}$  with respect to  $f_\theta$ :

$$v_q(i, \mathbf{x}_S) = \mathbb{E}_{p(x_i|\mathbf{x}_S)} [q(x_i, \mathbf{x}_S)]. \quad (6)$$

Function  $q(x_i, \mathbf{x}_S)$  combines two components: the predictive improvement from adding feature  $i$ , captured by  $u(\mathbf{x}_S \cup \{x_i\})$ , and the epistemic uncertainty of the resulting model, captured by  $e(\mathbf{x}_S \cup \{x_i\})$ :

$$q(x_i, \mathbf{x}_S) = u(\mathbf{x}_S \cup \{x_i\}) - \lambda e(\mathbf{x}_S \cup \{x_i\}). \quad (7)$$

The parameter  $\lambda$  regulates the relative importance of epistemic uncertainty in the DFS process.

To use this expression, we need to know:

- How to compute  $u$  using the global prediction and its effect on the behaviour of the DFS (Section 3.2.1).
- How to estimate  $e$ , for which we can use ensembles and also exploit some fuzzy logic properties when relevant (Section 3.2.2).
- As we cannot observe all features for a new sample, we need to estimate the  $v_q(i, \mathbf{x}_S)$  value in test time (Section 3.2.3).

To support variable feature costs, we divide  $v_q(x_i, \mathbf{x}_S)$  by the cost of the feature, so that the policy optimizes  $q$  it per unit cost. This is not an optimal solution Chen et al. [2015], but works well in practice and it is cheap to compute as well.

### 3.2.1 Difference Between Global and sub-Model Prediction

For computing the prediction difference of the sub-model defined by  $S$  with respect to the full model, we consider the Kullback–Leibler divergence of the model predictions:

$$u(\mathbf{x}_S) = D_{\text{KL}}(p(\hat{y}|\mathbf{x})||p(\hat{y}|\mathbf{x}_S)). \quad (8)$$

When an additional feature  $x_i$  is queried, this becomes:

$$u(\mathbf{x}_S \cup \{x_i\}) = D_{\text{KL}}(p(\hat{y}|\mathbf{x})||p(\hat{y}|\mathbf{x}_S \cup \{x_i\})). \quad (9)$$

We can show that this expression is minimized by the same  $x_i$  that maximizes the CMI, as long as the following proportionality holds:

$$I(x_i; \hat{y}|\mathbf{x}_S) \propto \mathbb{E}_{p(x_i|\mathbf{x}_S)} [u(\mathbf{x}_S) - u(\mathbf{x}_S \cup \{x_i\})]. \quad (10)$$

We provide a proof of this result in Appendix B. This shows that, although minimizing the disagreement with respect to the global model is closely related to the CMI and KL-based approaches in the literature (e.g., [Covert et al., 2023, Gadgil et al., 2023, Ma et al., 2018]), the two approaches are strictly equivalent only under the assumption that the subset of features considered already recovers the global model.

### 3.2.2 Epistemic uncertainty concerning Rule Firings

For crisp rules, we quantify epistemic uncertainty using auxiliary models, working similarly to ensembles for uncertainty quantification Rahaman et al. [2021]. This approach involves computing the predictions of a set of auxiliary classifiers,  $I$ , for the same sample. The final measure,  $e_R(\mathbf{x}_S)$ , is the average Kullback-Leibler Divergence between the original model’s winning rule prediction,  $p_{r^*}(\hat{y}|\mathbf{x}_S)$ , and the predictions of all auxiliary models,  $p_{r^*}^i(\hat{y}|\mathbf{x}_S)$ :

$$e_R(\mathbf{x}_S) = \frac{1}{|I|} \sum_{i \in I} D_{\text{KL}}(p_{r^*}^i(\hat{y} | \mathbf{x}_S) || p_{r^*}(\hat{y} | \mathbf{x}_S)). \quad (11)$$

Predictions with high confidence should exhibit little variation across models, resulting in low epistemic uncertainty.

For fuzzy rule-based models, the classical method for distinguishing between low and high confidence predictions is to compute the negation of the truth degree of the firing rule Shiraishi et al. [2025], which is a deterministic uncertainty approach Postels et al. [2022]. This expression, however, is problematic because it assumes that the probability  $p(y | \mu(r_A) = 1)$  is correctly estimated and that the confidence is solely dependent on the matching degree between the antecedent and the sample. Yet, the confidence of the rule can often be better calibrated for intermediate membership values (a further discussion on this can be found in Appendix C). Instead, we exploit the fact that in fuzzy systems multiple rules can fire simultaneously with varying degrees for the same sample. We define epistemic uncertainty as the membership-weighted divergence between all activated rules and the winning rule:

$$e_R(\mathbf{x}_S) = \sum_{r \in R} \mu_r(\mathbf{x}_S) D_{\text{KL}}(p_r(\hat{y}|\mathbf{x}_S) || p_{r^*}(\hat{y}|\mathbf{x}_S)). \quad (12)$$

where  $\mu_r(\mathbf{x}_S)$  denotes the firing strength of rule  $r$  for sample  $\mathbf{x}_S$ . This formulation eliminates the need for other auxiliary models using the weighted divergences against the predictions of other rules in the system.

### 3.2.3 Estimating the Value Function in Test Time

We train a neural estimator to approximate the value function  $v_q(i, \mathbf{x}_S)$  defined in Eq. (6), taking  $\mathbf{x}_S$  as input.

To jointly estimate both components of the value function, we train a single network with two heads: one for predicting the reduction in prediction discrepancy  $u$  and another for predicting the

reduction in epistemic uncertainty ( $e_R$ ). The training objective minimizes the prediction error for both components:

$$\min_{\phi} \sum_{i=1}^M \mathbb{E}_{\mathbf{x}_S} \mathbb{E}_{x_i} l(h_{u,i}(\mathbf{x}_S), u(\mathbf{x}_S \cup \{x_i\})) + l(h_{e,i}(\mathbf{x}_S), e_R(\mathbf{x}_S \cup \{x_i\})) \quad (13)$$

where  $l(a, b) = (a - b)^2$  is the squared error loss,  $h_{u,i}$  and  $h_{e,i}$  are the two heads of the neural estimator  $h$ , and  $\phi$  represents its parameters.

## 4 Experimentation

In our experiments, we validate our proposed approach for adapting rule-based models to DFS, assessing its predictive performance compared to other feature selection methods. We also compare how every method addresses the challenges discussed in Section 2.

### 4.1 Datasets and methods

For our experimentation, we use three clinical tabular datasets the clinical setting and two non-clinical ones:

- *Diabetes* dataset [Strack et al., 2014]: has 101766 samples and 47 features regarding patient condition. The target value is if the patient is readmitted in the hospital in a 30 day period after the last discharge.
- *Heart* disease [Detrano et al., 1989]: contains 13 clinical features for each of the 303 patients. The target field refers to the presence of heart disease in the patient which has been binarized into presence and absence.
- *Cirrhosis* Patient Survival Prediction [Fleming and Harrington, 2013]: uses 17 clinical features for predicting the survival state of 520 patients with liver cirrhosis. These include death, alive, or alive due to liver transplantation.
- *Wine*: the classical dataset containing chemical analysis results of wines [Aeberhard and Forina, 1992]. It includes 178 samples with 13 features, used for classification into wine types.
- *Yeast*: protein localization sites in yeast cells [Nakai, 1991]. It consists of 1,484 samples with 8 features, predicting the cellular compartment where a protein resides.

We compare against both static and dynamic feature selection approaches. For static selection, we include: (1) mutual information-based feature scoring with a decision tree model, (2) TabNet [Arik and Pfister, 2021], and (3) the concrete feature selector (CFS) [Balin et al., 2019]. For DFS, we evaluate: (1) CMI-based greedy optimization (DIME) [Covert et al., 2023], (2) variational greedy information pursuit (VIP) [Chattopadhyay et al., 2023], (3) Q-learning-based RL (CWCF) [Janisch et al., 2019], and (4) actor-critic networks (INVASE) [Yoon et al., 2018].

We evaluate our DFS adaptation method using two rule-based backbones as global models: CART decision trees [Breiman et al., 2017] and fuzzy decision trees using the FuzzyCART algorithm. Additional results using fuzzy rule-based classifiers are provided in Appendix D. Hyperparameter selection, replicability and tuning details for all methods are provided in Appendix E.

### 4.2 Results

**Accuracy Comparison.** Table 1 reports the average accuracy obtained using the first 10 features queried per sample and uniform costs. Our CART-DFS approach achieves the best overall performance with both the highest average accuracy (69.43%) and the best average rank (3.3) across datasets. It substantially outperforms neural-based DFS methods such as CWCF (64.96%) and INVASE (66.29%), and performs comparably to DIME (69.21%) while outperforming VIP (67.04%). Notably, static feature selection using CMI (69.25%) outperforms several DFS methods including CWCF, INVASE, and VIP, highlighting the difficulty of learning effective adaptive policies despite

Table 1: Accuracy comparison of Static and Dynamic Feature Selection methods. Results show the average accuracy after querying the first 10 features. The final rank is computed as the mean of the ranks obtained across the five individual datasets. Methods marked with \* are our proposed approaches.

Method		Diabetes	Heart	Cirrhosis	Wine	Yeast	Average (rank)
Static	CMI	64.04 ± 8.10	81.64 ± 11.63	64.60 ± 14.77	95.37 ± 2.54	45.59 ± 4.25	69.25(3.6)
	TabNet	55.20 ± 12.38	80.08 ± 10.22	66.58 ± 5.31	89.81 ± 3.07	53.21 ± 3.56	68.98(3.5)
	CFS	53.27 ± 4.90	71.31 ± 0.43	57.46 ± 3.15	92.22 ± 4.02	48.09 ± 9.37	64.47(6.8)
Dynamic	CWCF	55.78 ± 2.13	78.06 ± 10.19	59.28 ± 7.58	86.66 ± 5.05	45.03 ± 6.01	64.96(6.6)
	INVASE	54.10 ± 7.84	77.36 ± 3.92	61.19 ± 8.26	92.77 ± 1.57	46.03 ± 4.51	66.29(5.6)
	DIME	62.02 ± 1.86	81.75 ± 15.65	66.90 ± 9.04	89.81 ± 2.53	45.59 ± 1.15	69.21(3.6)
	VIP	63.12 ± 0.98	71.20 ± 5.39	66.34 ± 6.52	85.00 ± 3.53	49.53 ± 0.89	67.04(5.2)
	CART-DFS*	55.37 ± 0.32	78.68 ± 10.84	65.95 ± 5.59	95.37 ± 2.01	51.78 ± 3.08	69.43(3.3)
FuzzyCART-DFS*	53.91 ± 1.03	67.21 ± 10.07	66.40 ± 2.90	91.88 ± 5.72	50.16 ± 5.91	65.91(5.6)	

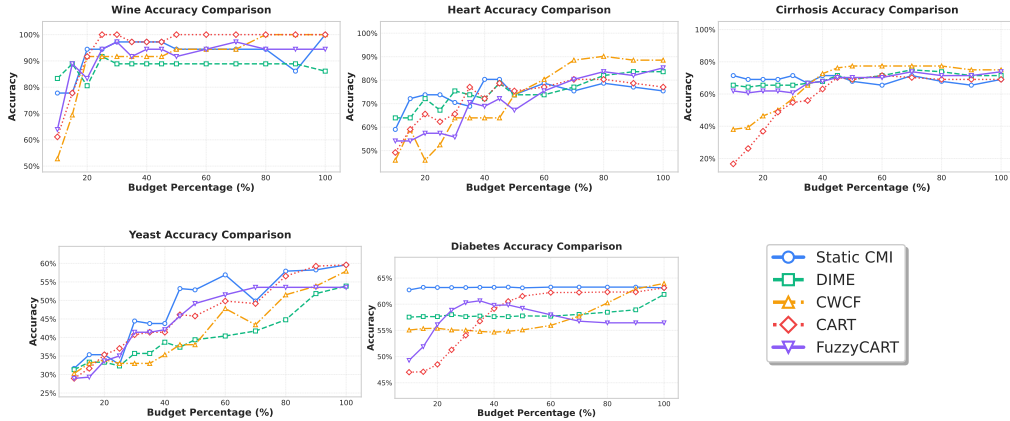


Figure 1: Performance comparison under varying feature costs and acquisition budgets for five tabular datasets.

the theoretical advantages of DFS. The FuzzyCART-DFS variant (65.91%) underperforms the crisp CART version, performing similarly to INVASE. This is partly due to the use of fixed fuzzy partitions, which can limit performance. RL-based methods like CWCF showed particular training instability, which lead to poorer performance than other greedy approaches.

Figure 1 shows the evolution in accuracy of five selected models for varying feature costs. These costs are randomly generated using a uniform distribution for each variable in the  $[1, 4]$  range, and remain the same in train and test time. Here, we can see that accuracy does not always increase monotonically with budget. It is true that there is a strong correlation between both, which is expected, but we can also see significant discrepancies. For instance, on the Diabetes dataset, FuzzyCART-DFS peaks at approximately 35% budget (60.66% accuracy) and then degrades significantly, dropping to 56.45% at full budget. We can also observe that dataset characteristics significantly influence relative performance. On Diabetes, all methods show relatively flat accuracy curves, with Static CMI maintaining a consistent lead throughout. This indicates that in some cases adaptive selection provides limited additional benefit. In contrast, on Cirrhosis and Heart, CART-DFS shows more gradual improvement, eventually matching or exceeding baselines at higher budgets. It is also worth pointing out that CWCF exhibits an interesting late-game advantage on several datasets (Wine, Heart, Yeast), where it starts poorly but catches up or surpasses other methods at 80-100% budget. This is an interesting case where we can see that when the  $\theta^*$  parameters are closer to the global model, performance gains at bigger budgets can be significant.

**Predictive uncertainty and calibration.** To analyse the confidence in model predictions, we analyze both the evolution of predictive entropy and calibration quality measured by Expected Calibration Error (ECE). ECE quantifies the alignment between predicted confidence and actual accuracy

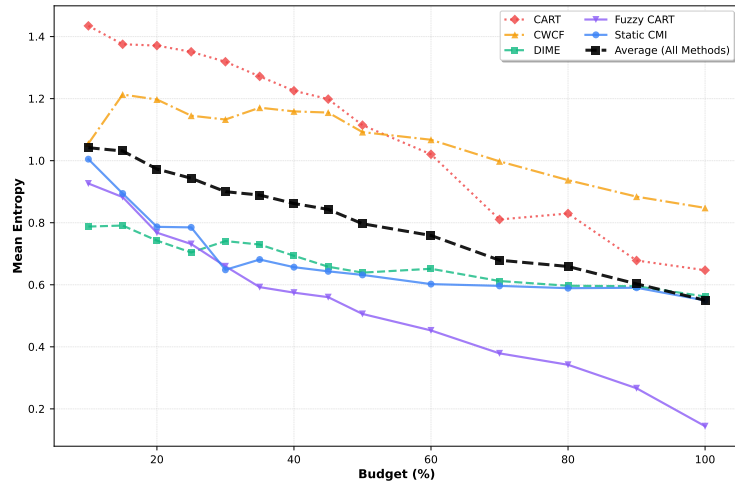


Figure 2: Average predictive entropy for each model in all tabular datasets tested, for increasing percentages of the total budget.

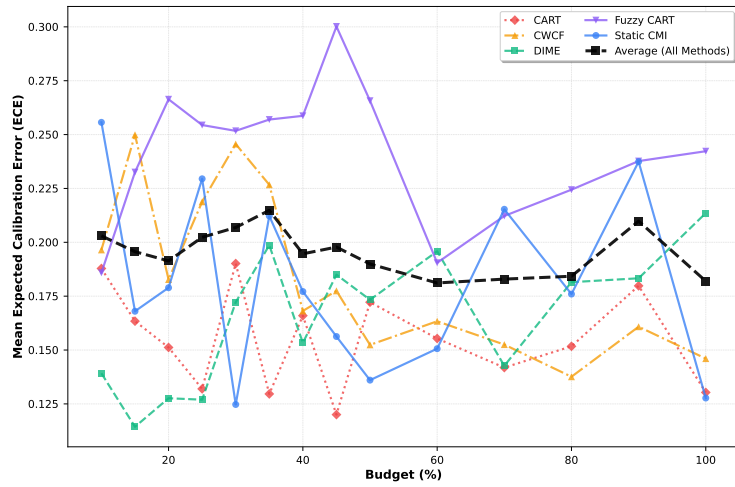


Figure 3: Evolution of average ECE for increasing budgets in all tabular datasets tested.

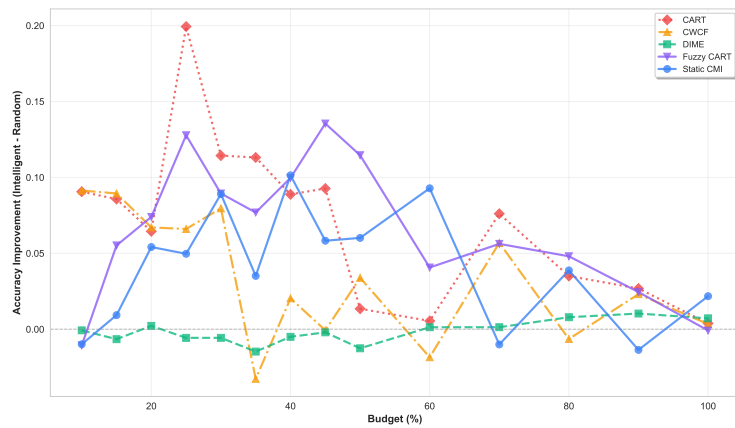


Figure 4: Evolution of average accuracy difference between feature selected and random masks for increasing budgets in the tabular datasets studied.

by partitioning predictions into equally-spaced confidence bins and measuring discrepancies:

$$\text{ECE} = \sum_{m=1}^M \frac{|B_m|}{n} |\text{acc}(B_m) - \text{conf}(B_m)|, \tag{14}$$

where  $B_m$  represents the  $m$ -th confidence bin,  $n$  is the total number of samples,  $\text{acc}(B_m)$  is the empirical accuracy within the bin, and  $\text{conf}(B_m)$  is the average predicted confidence Naeini et al. [2015]. All the tests were conducted using the variable feature costs setting.

As expected, we found that entropy generally decreases with additional features, but the rate and smoothness of this decline varies substantially across methods (Figure 2). Both CART-DFS and FuzzyCART-DFS show the smoothest entropy reduction, while DIME and the static CMI selection showed an almost non-existing reduction after 40% of budget. Most surprisingly, this entropy reduction pattern holds regardless if features are acquired using the trained policies or random selections. This suggests that the observed confidence growth is primarily driven by the accumulation of information rather than the specific order of acquisition. However, decreasing entropy does not guarantee improved calibration. The ECE analysis reveals no clear correlation between predictive entropy and calibration quality, nor between budget and ECE across methods (Figure 3). So, while models become more confident and accurate with additional features (Figure 1), this extra confidence might be unjustified in some cases.

**Model adaptability and Selector Usefulness.** Figure 4 shows the accuracy difference between using trained feature selection policies versus random feature masks at each budget level. This reveals how well each predictor model generalizes to unseen feature sets, and how much useful is the feature selector in each method. All the tree-based methods exhibited the biggest benefits from feature selection. This makes intuitive sense, as they are using a model that is not designed to handle arbitrary feature subsets robustly. For CWCF, we found significant gains up to 30% budget. However, after that point the behaviour seemed more erratic. Surprising, DIME offered no significant gains from its feature selection compared to random selection. This counterintuitive result suggests that DIME’s strong overall performance (Table 1) stems primarily from its base model’s robustness to different feature subsets rather than from learning an effective acquisition policy. We believe this may be a consequence of optimizing Eq. (1), which encourages the model to maintain good performance across various feature masks during training.

## 5 Conclusions and Future Lines

In this work we formalized how DFS introduces distinct sources of epistemic uncertainty beyond those present in static feature selection. We discuss that model adaptation to different feature subsets creates non-uniform uncertainty across the exponential feature, specially relevant when when training is guided by a jointly-learned selector that biases exploration toward a small subset of trajectories. Through theoretical analysis, we showed that how standard missing-value imputation techniques systematically biases classifier predictions. Moreover, we demonstrated that confidence-based stopping criteria can be unreliable in DFS settings, as predictive entropy tends to be reduced whether queried information is useful or not. We also discussed that in imbalanced classification problems high confidence may simply reflect base rate information rather than genuine certainty, which makes this stopping criteria also unreliable in such cases. Besides our theoretical analysis, we introduced a practical framework for DFS with interpretable predictions by adapting rule-based classifiers to operate on arbitrary feature subsets. Unlike existing neural-based DFS methods that produce opaque predictions, our approach ensures that final predictions remain transparent through rule-based reasoning. This is particularly valuable in high-stakes applications like clinical diagnosis, where DFS offers significant cost savings but prediction explainability is often a regulatory and ethical requirement.

We performed experiments on five real-world datasets spanning clinical and non-clinical domains. Our rule-based DFS achieved accuracy comparable to state-of-the-art neural and greedy methods while providing interpretable predictions through transparent rule-based reasoning. Beyond accuracy metrics, our uncertainty analysis revealed several findings that challenge common assumptions in DFS. First, predictive entropy decreases with feature acquisition, at same ratio whether features are selected intelligently or randomly. However, this confidence growth does not translate to improved calibration. The ECE analysis showed no correlation between budget and calibration quality

across methods, with some models exhibiting better calibration on smaller feature subsets than larger ones. This indicates that DFS models become more confident without necessarily becoming more reliable, a significant concern for risk-sensitive applications. Second, our analysis revealed that the value of learned selection policies varies dramatically: tree-based methods show substantial gains from intelligent feature acquisition, while other methods performance stems primarily from predictor robustness rather than effective feature selection. The the latter case, the model achieves in a nice uniform distribution of the epistemic uncertainty across all feature subsets, at the cost of making the feature selector almost redundant.

## 6 Acknowledgments

This research and Javier Fumanal-Idocin were supported by EU Horizon Europe under the Marie Skłodowska-Curie COFUND grant No 101081327 YUFE4Postdocs.

Raquel Fernandez-Peralta is funded by the EU NextGenerationEU through the Recovery and Resilience Plan for Slovakia under the project No. 09I03-03-V04- 00557.

## References

- Stefan Aeberhard and M. Forina. Wine. UCI Machine Learning Repository, 1992. DOI: <https://doi.org/10.24432/C5PC7J>.
- Sercan Ö Arik and Tomas Pfister. Tabnet: Attentive interpretable tabular learning. In *Proceedings of the AAAI conference on artificial intelligence*, volume 35, pages 6679–6687, 2021.
- Muhammed Fatih Balın, Abubakar Abid, and James Zou. Concrete autoencoders: Differentiable feature selection and reconstruction. In *International conference on machine learning*, pages 444–453. PMLR, 2019.
- Leo Breiman, Jerome Friedman, Richard A Olshen, and Charles J Stone. *Classification and regression trees*. Chapman and Hall/CRC, 2017.
- Aditya Chattopadhyay, Kwan Ho Ryan Chan, Benjamin David Haeffele, Donald Geman, and Rene Vidal. Variational information pursuit for interpretable predictions. In *The Eleventh International Conference on Learning Representations*, 2023.
- Yuxin Chen, S Hamed Hassani, Amin Karbasi, and Andreas Krause. Sequential information maximization: When is greedy near-optimal? In *Conference on Learning Theory*, pages 338–363. PMLR, 2015.
- Ian Connick Covert, Wei Qiu, Mingyu Lu, Na Yoon Kim, Nathan J White, and Su-In Lee. Learning to maximize mutual information for dynamic feature selection. In *International Conference on Machine Learning*, pages 6424–6447. PMLR, 2023.
- Robert C. Detrano, András Jánosi, Walter Steinbrunn, Matthias Emil Pfisterer, Johann-Jakob Schmid, Sarbjit Sandhu, Kern Guppy, Stella Lee, and Victor Froelicher. International application of a new probability algorithm for the diagnosis of coronary artery disease. *The American journal of cardiology*, 64 5:304–10, 1989. URL <https://api.semanticscholar.org/CorpusID:23545303>.
- Gabriel Erion, Joseph D Janizek, Carly Hudelson, Richard B Utarnachitt, Andrew M McCoy, Michael R Sayre, Nathan J White, and Su-In Lee. A cost-aware framework for the development of ai models for healthcare applications. *Nature Biomedical Engineering*, 6(12):1384–1398, 2022.
- Chelsea Finn, Pieter Abbeel, and Sergey Levine. Model-agnostic meta-learning for fast adaptation of deep networks. In Doina Precup and Yee Whye Teh, editors, *Proceedings of the 34th International Conference on Machine Learning*, volume 70 of *Proceedings of Machine Learning Research*, pages 1126–1135. PMLR, 2017.
- Thomas R Fleming and David P Harrington. *Counting processes and survival analysis*. John Wiley & Sons, 2013.

- Javier Fumanal Idocin and Javier Andreu-Perez. Ex-fuzzy: A library for symbolic explainable ai through fuzzy logic programming. *Neurocomputing*, 2024.
- Soham Gadgil, Ian Connick Covert, and Su-In Lee. Estimating conditional mutual information for dynamic feature selection. In *The Twelfth International Conference on Learning Representations*, 2023.
- David Ha, Andrew M. Dai, and Quoc V. Le. Hypernetworks. In *International Conference on Learning Representations*, 2017.
- Eyke Hüllermeier and Willem Waegeman. Aleatoric and epistemic uncertainty in machine learning: An introduction to concepts and methods. *Machine learning*, 110(3):457–506, 2021.
- Jaromír Janisch, Tomáš Pevný, and Viliam Lisý. Classification with costly features using deep reinforcement learning. In *Proceedings of the AAAI conference on artificial intelligence*, volume 33, pages 3959–3966, 2019.
- David Krueger, Ethan Caballero, Joern-Henrik Jacobsen, Amy Zhang, Jonathan Binas, Dinghui Zhang, Remi Le Priol, and Aaron Courville. Out-of-distribution generalization via risk extrapolation (rex). In Marina Meila and Tong Zhang, editors, *Proceedings of the 38th International Conference on Machine Learning*, volume 139 of *Proceedings of Machine Learning Research*, pages 5815–5826. PMLR, 2021.
- Jundong Li, Kewei Cheng, Suhang Wang, Fred Morstatter, Robert P Trevino, Jiliang Tang, and Huan Liu. Feature selection: A data perspective. *ACM computing surveys (CSUR)*, 50(6):1–45, 2017.
- Kunpeng Liu, Yanjie Fu, Le Wu, Xiaolin Li, Charu Aggarwal, and Hui Xiong. Automated feature selection: A reinforcement learning perspective. *IEEE Transactions on Knowledge and Data Engineering*, 35(3):2272–2284, 2021.
- Chao Ma, Sebastian Tschitschek, Konstantina Palla, José Miguel Hernández-Lobato, Sebastian Nowozin, and Cheng Zhang. Eddi: Efficient dynamic discovery of high-value information with partial vae. *arXiv preprint arXiv:1809.11142*, 2018.
- Prem Melville, Maytal Saar-Tsechansky, Foster Provost, and Raymond Mooney. Active feature-value acquisition for classifier induction. In *Fourth IEEE International Conference on Data Mining (ICDM'04)*, pages 483–486. IEEE, 2004.
- Mahdi Pakdaman Naeini, Gregory Cooper, and Milos Hauskrecht. Obtaining well calibrated probabilities using bayesian binning. In *Proceedings of the AAAI conference on artificial intelligence*, volume 29, 2015.
- Kenta Nakai. Yeast. UCI Machine Learning Repository, 1991.
- Sarah Nogueira, Konstantinos Sechidis, and Gavin Brown. On the stability of feature selection algorithms. *Journal of Machine Learning Research*, 18(174):1–54, 2018.
- Harrie Oosterhuis, Lijun Lyu, and Avishek Anand. Local feature selection without label or feature leakage for interpretable machine learning predictions. In *Proceedings of the 41st International Conference on Machine Learning*, pages 38740–38761, 2024.
- Janis Postels, Mattia Segù, Tao Sun, Luca Daniel Sieber, Luc Van Gool, Fisher Yu, and Federico Tombari. On the practicality of deterministic epistemic uncertainty. In *International Conference on Machine Learning*, pages 17870–17909. PMLR, 2022.
- Rahul Rahaman et al. Uncertainty quantification and deep ensembles. *Advances in neural information processing systems*, 34:20063–20075, 2021.
- Samrudhdi B Rangrej and James J Clark. A probabilistic hard attention model for sequentially observed scenes. *arXiv preprint arXiv:2111.07534*, 2021.
- Sylvestre-Alvise Rebuffi, Andrea Vedaldi, and Hakan Bilen. Efficient parametrization of multi-domain deep neural networks. In *2018 IEEE/CVF Conference on Computer Vision and Pattern Recognition*, pages 8119–8127, 2018.

- Noam Shazeer, \*Azalia Mirhoseini, \*Krzysztof Maziarz, Andy Davis, Quoc Le, Geoffrey Hinton, and Jeff Dean. Outrageously large neural networks: The sparsely-gated mixture-of-experts layer. In *International Conference on Learning Representations*, 2017.
- Hiroki Shiraishi, Hisao Ishibuchi, and Masaya Nakata. A class inference scheme with dempster-shafer theory for learning fuzzy-classifier systems. *ACM Transactions on Evolutionary Learning*, 2025.
- Beata Strack, Jonathan P DeShazo, Chris Gennings, Juan L Olmo, Sebastian Ventura, Krzysztof J Cios, and John N Clore. Impact of hba1c measurement on hospital readmission rates: analysis of 70,000 clinical database patient records. *BioMed research international*, 2014(1):781670, 2014.
- Katsumi Takahashi, Koh Takeuchi, and Hisashi Kashima. Dynamic feature selection from variable feature sets using features of features. *arXiv preprint arXiv:2503.09181*, 2025.
- Jinsung Yoon, James Jordon, and Mihaela Van der Schaar. Invase: Instance-wise variable selection using neural networks. In *International conference on learning representations*, 2018.

## Appendix

### A Adapting classical heuristics in rule-learning for DFS

In this paper we are using three different rule-classification training algorithms: CART, FuzzyCART, which are greedy optimization algorithms; and genetic fine tuning.

The aim in CART for classification is to find the split  $\theta$  (on feature  $m$  and threshold  $t$ ) that maximizes the purity gain, typically measured by the decrease in Gini Impurity. At a node, the Gini Impurity is defined as:

$$I_G(X) = 1 - \sum_{k=1}^K p_k^2 \quad (15)$$

where  $p_k$  is the proportion of class  $k$  in  $X$ . The quality of a split  $\theta$  that partitions  $X$  into  $X_{\text{left}}$  and  $X_{\text{right}}$  is:

$$\Delta I_G(X) = I_G(X) - \left( \frac{|X_{\text{left}}|}{|X|} I_G(X_{\text{left}}) + \frac{|X_{\text{right}}|}{|X|} I_G(X_{\text{right}}) \right). \quad (16)$$

The optimal split is then selected as:

$$\arg \max \Delta I_G(D, \theta) \quad (17)$$

In DFS, we need to take into account that we are not observing the  $X$ , but only a subset of features every time, so we just need to use the expectation operator to obtain the best split on average for every subset of features. So, if the split is happening in feature  $j$ , the expression to minimize is the following:

$$\mathbb{E}_{\{S \in \mathcal{P}(\mathbf{s}): j \in A\}} \arg \max_{\theta} \Delta I_G(X_S, \theta), \quad (18)$$

For FuzzyCART and the genetic optimization, the adaption is analogous.

### B Equivalence between Prediction Similarity minimization and CMI

First of all, we prove the following equality regarding the difference between the aleatoric uncertainty of considering an additional feature to the already considered set  $S$ .

**Lemma 1.**

$$\Delta u_i = - \sum_{\hat{y}} p(\hat{y} | \mathbf{x}) \log \left( \frac{p(\hat{y} | \mathbf{x}_S, x_i)}{p(\hat{y} | \mathbf{x}_S)} \right),$$

where  $\Delta u_i = u(\mathbf{x}_S \cup \{x_i\}) - u(\mathbf{x}_S)$ .

*Proof.*

$$\begin{aligned} u(\mathbf{x}_S \cup \{x_i\}) &= \sum_{\hat{y}} p(\hat{y} | \mathbf{x}) \log \left( \frac{p(\hat{y} | \mathbf{x})}{p(\hat{y} | \mathbf{x}_S, x_i)} \right) \\ &= \sum_{\hat{y}} p(\hat{y} | \mathbf{x}) \log \left( \frac{p(\hat{y} | \mathbf{x})}{p(\hat{y} | \mathbf{x}_S, x_i)} \right) \\ &\quad \pm \sum_{\hat{y}} p(\hat{y} | \mathbf{x}) \log(p(\hat{y} | \mathbf{x}_S)) \\ &= u(\mathbf{x}_S) + \sum_{\hat{y}} p(\hat{y} | \mathbf{x}) \log \left( \frac{p(\hat{y} | \mathbf{x}_S)}{p(\hat{y} | \mathbf{x}_S, x_i)} \right). \end{aligned}$$

□

Now, suppose we assume that the partial models produce predictions that are proportional to those of the global model. In that case, we can show that the CMI is also proportional to the expected reduction in aleatoric uncertainty.

**Proposition 1.** *If  $p(\hat{y} | \mathbf{x}) \propto p(\hat{y} | \mathbf{x}_S, x_i)$  then*

$$-\mathbb{E}_{p(x_i | \mathbf{x}_S)}[\Delta u_i] \propto I(x_i; \hat{y} | \mathbf{x}_S).$$

*Proof.* According to Lemma 1 we have

$$\Delta u_i = - \sum_{\hat{y}} p(\hat{y} | \mathbf{x}) \log \left( \frac{p(\hat{y} | \mathbf{x}_S, x_i)}{p(\hat{y} | \mathbf{x}_S)} \right).$$

If  $p(\hat{y} | \mathbf{x}) \propto p(\hat{y} | \mathbf{x}_S, x_i)$  then

$$\Delta u_i \propto -p(\hat{y} | \mathbf{x}_S, x_i) \log \left( \frac{p(\hat{y} | \mathbf{x}_S, x_i)}{p(\hat{y} | \mathbf{x}_S)} \right)$$

Now, since  $p(x_i, \hat{y} | \mathbf{x}_S) = p(\hat{y} | \mathbf{x}_S, x_i)p(x_i | \mathbf{x}_S)$  we have that

$$\Delta u_i \propto -\frac{p(x_i, \hat{y} | \mathbf{x}_S)}{p(x_i | \mathbf{x}_S)} \log \left( \frac{p(\hat{y} | \mathbf{x}_S, x_i)}{p(\hat{y} | \mathbf{x}_S)} \right).$$

Since,

$$I(x_i; \hat{y} | \mathbf{x}_S) = \sum_{x_i, \hat{y}} p(x_i, \hat{y} | \mathbf{x}_S) \log \left( \frac{p(\hat{y} | \mathbf{x}_S, x_i)}{p(\hat{y} | \mathbf{x}_S)} \right),$$

we have obtained the desired result.  $\square$

Thus, in this case, the next feature obtained by minimizing the expected aleatoric uncertainty coincides with the one selected by those methods that maximize the CMI. This shows that our methodology is only equivalent to those methods in the case of already having a feature subset that recovers the global model.

**Corollary 1.** *If  $p(\hat{y} | \mathbf{x}) \propto p(\hat{y} | \mathbf{x}_S, x_i)$  then*

$$\arg \min_{i \in \bar{S}} \mathbb{E}_{p(x_i | \mathbf{x}_S)}[u(x_S \cup \{x_i\})] = \arg \max_{i \in \bar{S}} I(x_i; \hat{y} | \mathbf{x}_S).$$

## C Rule Confidence Calibration

The calibration error of fuzzy rule confidence estimates varies as a function of membership degree  $\mu_r(\mathbf{x})$ , which may not occur at maximal membership ( $\mu_r(\mathbf{x}) = 1$ ) but rather at intermediate membership values.

For rule  $r : r_A \Rightarrow c$ , the fuzzy support is defined as:

$$\text{Support}(r_A) = \frac{\sum_{\mathbf{x} \in \mathcal{D}} \mu_r(\mathbf{x})}{|\mathcal{D}|}, \quad (19)$$

and the rule confidence is:

$$\text{Confidence}(r) = \frac{\sum_{\mathbf{x} \in \mathcal{D}} \mu_r(\mathbf{x}) \mathbb{I}(y(\mathbf{x}) = c)}{\sum_{\mathbf{x} \in \mathcal{D}} \mu_r(\mathbf{x})}. \quad (20)$$

To analyse calibration, we partition the data by membership degree intervals. For interval  $I_k = [\mu_{k-1}, \mu_k]$ , let  $\mathcal{D}_{k,r} = \{\mathbf{x} \in \mathcal{D} : \mu_r(\mathbf{x}) \in I_k\}$ . The empirical confidence at membership level  $k$  is:

$$\text{Confidence}_k(r) = \frac{\sum_{\mathbf{x} \in \mathcal{D}_{k,r}} \mu_r(\mathbf{x}) \mathbb{I}(y(\mathbf{x}) = c)}{|\mathcal{D}_{k,r}|}. \quad (21)$$

However, the predicted confidence for samples in  $\mathcal{D}_{k,r}$  when using the global rule confidence is still  $\text{Confidence}(r)$ . Moreover, we can see that the global confidence is a weighted average of local confidences:

$$\text{Confidence}(r) = \sum_k \frac{\sum_{\mathbf{x} \in \mathcal{D}_{k,r}} \mu_r(\mathbf{x}) \mathbb{I}(y(\mathbf{x}) = c)}{\sum_{\mathbf{x} \in \mathcal{D}} \mu_r(\mathbf{x})}. \quad (22)$$

This means  $\text{Confidence}(r)$  will be closest to  $\text{Confidence}_k(r)$  for membership levels  $k$  that have the highest weight in the fraction. For example, if the membership distribution is skewed toward lower values, the confidence will be best calibrated for those regions with the highest membership-weighted representation, not necessarily at  $\mu_r(\mathbf{x}) = 1$ .

## D Results with a genetic fine-tuned fuzzy rule base

For using fuzzy rule-based classifiers (FRBCs), we fitted with a genetic algorithm that employs the Matthew Correlation Coefficient as a fitness function [Fumanal Idocin and Andreu-Perez, 2024]. Due to the expensive training process of the genetic algorithm, results for FRBCs are only computed for the three smallest datasets: *Cirrhosis*, *Heart*, and *Wine*.

(Figure 5) We tried the fuzzy rule-based classifier (FRBC) method on three datasets only, as the computational cost of fitting the genetic algorithm to fit the fuzzy rules is prohibitive for larger datasets. Performance-wise, the FRBC is less accurate, though it is also the one with the shortest rules, and has the lowest number of rules in *Cirrhosis* and *Heart* by a significant margin (Table 2). Regarding performance evolution, the FRBC required more features to improve the accuracy, while CART had a better progression. The evolution of the prediction uncertainty was also smoother in CART. Epistemic uncertainty, however, is not so easily reduced as prediction uncertainty. For example, in the *Heart* dataset, epistemic uncertainty remains high until 50% of the features have been collected. However, a strong correlation between the two is observed in all cases.

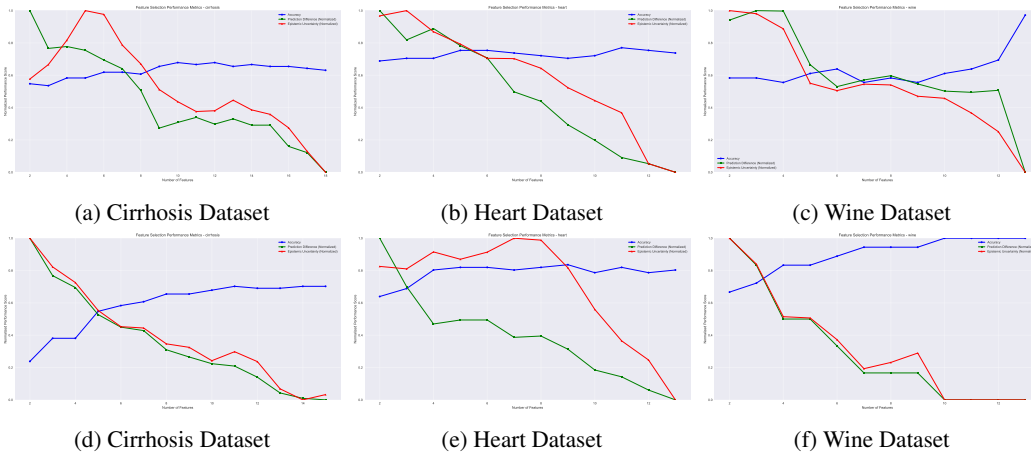


Figure 5: Results for Dynamic Feature Selection using fuzzy rule-based classification (top row) and CART (bottom row). The blue line is accuracy, the green one is prediction uncertainty, and the red one is epistemic uncertainty.

Table 2: Complexity comparison between fuzzy rule-based and CART. ACL stands for Average Condition Length

Dataset	Method	Acc.	Rules	ACL	Complexity
Cirrhosis	CART	72.41	47	7.09	333.23
	FRBC	73.81	18	1.27	22.86
Heart	CART	75.55	35	5.65	197.75
	FRBC	73.77	10	1.60	16.00
Wine	CART	98.77	12	2.13	24.26
	FRBC	96.30	16	1.62	25.92

Table 3: Dataset Summary

Dataset	Samples	Features	Classes	Acc. LR
Diabetes	101,766	47	2	0.61
Heart	303	13	2	0.86
Cirrhosis	520	17	3	0.72
Wine	178	13	3	0.98
Yeast	1,484	8	10	0.57

## E Reproducibility: Hyperparameter selection and model architectures

All code, including custom implementations of dynamic feature selection methods, neural estimators, and evaluation frameworks, will be made publicly available upon publication.

A summary of the classification datasets’ size and properties is in Table 3. We also included the performance of a logistic regressor for each one as a baseline reference.

Our neural estimator proposed in Section 5.4 uses the following parameters:

- **Architecture:** 2-layer MLP with adaptive hidden size  $\min(64, \text{feature\_size} \times 2)$
- **Activation:** SELU with dropout rate 0.5
- **Training:** 100 epochs (comparison), 10 epochs (individual), learning rate 0.01, Adam optimizer
- **Regularization:** L1 weights tested [0.0, 0.001, 0.01, 0.1, 0.5, 1.0, 2.0]

The hyperparameters for the backbone classifiers for our DFS proposal are:

- **Decision Tree:** maximum depth of 10, minimum of 5 samples for a split, a minimum of 2 samples to generate a leaf.
- **Random Forest:** 100 estimators, same depth parameters as Decision Tree.
- **MLP:** hidden layer sizes of 100, with two hidden layers. We use a ReLU activation. We use an Adam optimizer with 200 iterations.

## F Discarding Features in the Search Space

The output of a rule-based classifier is determined by:

$$\hat{y} = c, \quad \text{where } r^* = \arg \max_{r \in R} r(\mathbf{x})$$

where  $c$  denotes the consequent of rule  $r^*$ . A key property emerges from the conjunctive nature of rule antecedents; the truth value of any rule  $r$  is bounded by its weakest condition:

$$r(\mathbf{x}) \leq \min_{t \in r_A} t(\mathbf{x})$$

where  $r_A$  is the set of conditions in the antecedent of rule  $r$ . This bound enables efficient search space reduction through two mechanisms:

1. Early termination: if any condition  $t(\mathbf{x})$  evaluates to 0 (completely false), we can immediately discard rule  $r$  without evaluating remaining conditions. We can also set that value to an arbitrary threshold  $\theta > 0$ , which can be especially useful when working with fuzzy logic conditions.
2. Feature selection: the active feature space can be reduced to:

$$S_{active} = \bigcup_{\substack{r \in R \\ r(\mathbf{x}_S) > \theta}} \bigcup_{t \in r_A} \text{feature}(t)$$

where  $\text{feature}(t)$  denotes index of the feature involved in condition  $t$ .

This optimization significantly reduces computational complexity while preserving the exactness of the rule evaluation process.